Наносистеми, наноматеріали, нанотехнології
Nanosistemi, Nanomateriali, Nanotehnologii
2026, т. 24, № 1, сс. 249–265
https://doi.org/10.15407/nnn.24.01.0249

© 2026 ІМФ (Інститут металофізики
ім. Г. В. Курдюмова НАН України)
Надруковано в Україні.

PACS numbers: 07.07.Vx, 68.37.Hk, 68.37.Vj, 68.55.J-, 72.80.Tm, 78.20.Ci, 78.67.Sc

The Effect of Increasing ZnO Nanomaterial in PVA–ZnO Nanocomposites and Investigating Some of Their Properties for Utilization as Humidity Sensor

Ameen Alwan Mohaimeed[1,2] and Maher Hassan Rasheed[3]

[1]*College of Sciences,*
Medical Physics Department,
Al-Mustaqbal University,
51001 Babil, Iraq
[2]*Directorate of Education Babylon,*
Ministry of Education,
Homs, Iraq
College of Basic Education,
[3]*Department of Science,*
University of Babylon,
Hilla, Iraq

This research is aimed to prepare PVA with ratios of 0.2, 0.4, and 0.6 wt.% by the casting method and with a thickness of 270±5 μm. The morphological characteristics are examined *via* FE–SEM and FT–IR, and the results show that the composites have a homogeneous and granular structure and that ZnO is well distributed within the polymer. The reason for the increased movement of charges is the action of a grid of nanomaterials inserted into the polymer. FT–IR analysis reveals absorption peaks at 3251.3 cm^{-1} and 2812 cm^{-1} due to the O–H bond, which indicates the presence of polyvinyl alcohol. The absorbance of the prepared composites increases with increasing nanomaterials' concentration, reaching 93% at 6 wt.%. In addition, the energy gap decreases with increasing nanomaterial concentration to 2.87–2.73 eV, and all optical parameters α, n, k, ε_r, and ε_i increase with increasing nanomaterials' concentration. For all the samples, the dielectric constant decreases as the frequency increases and increases with increasing nanomaterials' concentration within the polymer. A decrease in the effect of charge polarization is the main factor of the dielectric loss of the PVA–ZnO nanocomposite; at the same time, increasing the concentration of nanomaterials leads to an increase in the dielectric loss. An increase in the frequency of the electric field and an increase in the concentration of nanomaterials increase the electrical conductivity. The humidity sensor shows almost no humidity hysteresis, and its resistance decreases with increasing humidity and zinc-oxide concentration.

This makes these films useful for electronic applications and light filters, and they can be also used as ultraviolet detectors and humidity sensors.

Це дослідження має на меті приготування полівінілового спирту (ПВС) зі співвідношенням компонентів 0,2, 0,4 та 0,6 мас.% методом лиття та товщиною у 270±5 мкм. Морфологічні характеристики досліджено за допомогою емісійної (автоелектронної) сканувальної електронної мікроскопії та інфрачервоної спектроскопії на основі Фур'є-перетвору; результати показали, що композити мають однорідну та зернисту структуру, а ZnO добре розподілений у полімері. Причиною посиленого руху зарядів є дія сітки наноматеріялів, вставлених у полімер. Аналіза даних інфрачервоної спектроскопії на основі Фур'є-перетвору виявила піки вбирання в околі 3251,3 $см^{-1}$ і 2812 $см^{-1}$, зумовлені зв'язком O–H, що вказує на наявність полівінілового спирту. Вбирання одержаних композитів збільшується зі збільшенням концентрації наноматеріялів, досягнувши 93% за 6 мас.%. Крім того, заборонена енергетична зона зменшується зі збільшенням концентрації наноматеріялів до 2,87–2,73 еВ, а всі оптичні параметри α, n, k, ε_r і ε_i збільшуються зі збільшенням концентрації наноматеріялів. Для всіх зразків діелектрична проникність зменшується зі збільшенням частоти та збільшується зі збільшенням концентрації наноматеріялів у полімері. Зменшення впливу поляризації заряду є основним чинником діелектричних втрат нанокомпозиту ПВС–ZnO; водночас збільшення концентрації наноматеріялів призводить до збільшення діелектричних втрат. Підвищення частоти електричного поля та збільшення концентрації наноматеріялів підвищують електропровідність. Датчик вологости майже не демонструє гістерези вологости, а його опір зменшується з підвищенням вологости та концентрації оксиду Цинку. Це робить зазначені плівки корисними для електронних застосувань і світлофільтрів, а також їх можна використовувати як ультрафіолетові детектори та датчики вологости.

Key words: PVA–ZnO nanocomposites, a.c. electrical properties, morphological properties, zinc oxide, humidity sensor.

Ключові слова: нанокомпозити полівініловий спирт–ZnO, електричні властивості на змінному струмі, морфологічні властивості, оксид Цинку, датчик вологости.

(Received 5 August, 2024)

1. INTRODUCTION

Composite materials are composed of two or more phases that are different from one another both chemically and physically [1]. These amazing materials, sometimes referred to as nanocomposites, are an integral part of contemporary materials due to their many advantages, which include low weight, resistance to corrosion, high fatigue strength, and simple assembly [2]. When creating compos-

ites, reinforcing material is often added in a continuous phase called the matrix or binder [3]. Strengthening and enhancing overall properties are frequently achieved by incorporating dispersed phases into the matrix, which may be an engineered material such as a metal, polymer, or ceramic [4].

Nanocomposites do not differ from traditional materials in terms of the filling and matrix, but traditionally, they use, for example, glass or carbon fibres [5], while nanocomposites use a filling made of nanomaterial such as gold, silver, and silicon [2]. The composite depends upon three factors: the matrix, the reinforcement, and the adherence of the matrix to the reinforcement [6], compatibility and the ability to dissolve in water. In addition, hydrogels can be formed by physical and chemical methods [7]. Polyvinyl alcohol (PVA) has features that have made it the focus of researchers' attention due to its strong storage and insulating ability and its optical and electrical properties depending on the activator [8, 9]. PVA, with the formula $(C_2H_4O)_n$, is frequently used in various contexts, with semiconductors being one of the most prevalent [10]. The semiconductor zinc oxide (ZnO) has a large exciton binding energy of 60 meV at ambient temperature and relatively wide band-gap energy of 3.37 eV [11].

For use in medicine and the environment, ZnO is also biocompatible, biodegradable, and biosafe [11, 12]. The energy gap of ZnO is wide, making it one of the most promising semiconductor materials for optical applications in the ultraviolet spectral range [13]. The process of doping polymers and forming a matrix is beneficial for the formation of nanocomposites, and as a result, the structural and other physical properties increase [14], the fabrication of polymer-based nanocomposites for investment in electronic and optical applications and solar cells [15, 16]. This work investigated the morphological, electrical, and optical properties of PVA–ZnO nanocomposites *via* FE–SEM, optical microscopy, and FT–IR spectroscopy. This research aims to create PVA–ZnO nanocomposites and analyze their electrical and optical properties, as well as some structural aspects, with the intention of employing them as humidity sensors.

2. COMPUTATIONAL DETAILS

This section concentrates on the procedural aspects of employing the casting process to produce and examine PVA–ZnO. 25 ml of distilled water was used to dissolve 1 g of PVA, and after the polymer was completely dissolved, a percentage of 0, 2, 4 and 6 wt.% ZnO were added. Then, the nanomaterial was dispersed with an ultrasonic device. After that, the mixture was poured into dishes to a thickness of 270 ± 5 μm. After one week, these films were measured.

Zinc oxide (ZnO): Zhengzhou Dongyao Nano Materials Co., Ltd., is a Chinese company, from which this powder was obtained. Its features include a high purity of 99.99%, a white colour, a density of 5.606 g/cm^3, and a nanoparticle size of 50 nm.

The molecular weight of the utilized polyvinyl alcohol (PVA) ranged from 26.200 to 30.400 g/mol. China's Shanghai Kaidu Industrial Development Co., Ltd. is the manufacturer of PVA.

The optical properties of the films, such as the absorbance (A), absorbance coefficient (α), real dielectric constant (ε_r), imaginary dielectric constant (ε_i), refractive index (n), extinction coefficient (k) and band gab (E_g), were evaluated *via* several measurements. These measurements were conducted using a spectrophotometer equipped with two laser beams Shimadzu, UV-1800 A0, Japan across the spectrum range of 200 nm to 1100 nm. The structural characteristics of the PVA–ZnO films were investigated by Fourier transform infrared (FT–IR) spectroscopy in the range of 500–4000 cm^{-1} and FE–SEM, and the results were analyzed. Additionally, the electrical properties of the a.c. films were examined and analyzed.

Understanding a material's optical constants in great detail across a broad range of wavelengths is necessary for its use in optical applications and the creation of reflective coatings [17]. The optical characteristics of all materials may be correlated with their electrical, electronic band, and atomic structures [18]. The Beer–Lambert equation is the equation, by which the optical absorption coefficient can be described [19]:

$$\alpha = \frac{2.303A}{t}. \tag{1}$$

The logarithmic relationship between the incident intensity I_0 and the reflected I_A is known as the absorbance A [20]:

$$A = -\log T_r = \log\left(\frac{I_0}{I_A}\right). \tag{2}$$

Optical constants of the optical properties of films, such as the complex dielectric constant (with parts ε_r, ε_i), extinction coefficient (k), and index of refraction (n), can be described as follow [21]:

$$k = \frac{\alpha\lambda}{4\pi}, \tag{3}$$

$$n = \frac{1 + R_{1/2\,0}}{1 - R_{1/2\,0}}. \tag{4}$$

Through these two equations, complex dielectric constants can be

calculated as follow [22]:

$$\varepsilon_r = n^2 - k^2, \tag{5}$$

$$\varepsilon_i = 2nk. \tag{6}$$

The optical energy gap can be determined from that region as shown in the following relationship [23]:

$$\alpha h\nu = \beta\left(h\nu - E_g\right)^r. \tag{7}$$

The presence of free ions in the polymer increases its electrical conductivity:

$$\sigma_v = \frac{1}{\rho_v} = \frac{L}{R_V A_r}. \tag{8}$$

Using the Debye equation, the dielectric constant can be calculated:

$$\varepsilon = \varepsilon' - i\varepsilon'', \tag{9}$$

where ε'' represents the dielectric loss [24].

3. RESULTS AND DISCUSSION

3.1. Optical Properties

Figure 1 shows the absorption for samples with a thickness of 270 ± 5 μm. The absorption in the ultraviolet region is high and begins to decrease at a wavelength of 400 nm. Additionally, with increasing concentrations of the ZnO nanomaterial, the absorption decreases even with increasing wavelength, and the absorbance reaches 93% at 6 wt.% [25]. The absorption coefficient can be calculated from Eq. (1). Figure 2 shows that with increasing energy, the absorption coefficient increases, and the type of electronic transitions can be determined. This increase is due to an increase in the concentration of ZnO, which leads to electronic crossing between the partial orbitals with the help of phonons, and the electronic momentum is preserved [8, 26]. It is possible to draw a tangent slope for all the films, which shows the energy gap *versus* the photon energy. The results also showed that by increasing the concentration of nanomaterials ZnO, the energy gap decreases, which explains the narrowing of the crossing region from the valence band to the conduction band and the increase in the movement of electrons [27].

Figure 3 shows that the energy gap decreased as 2.87, 2.83, 2.79,

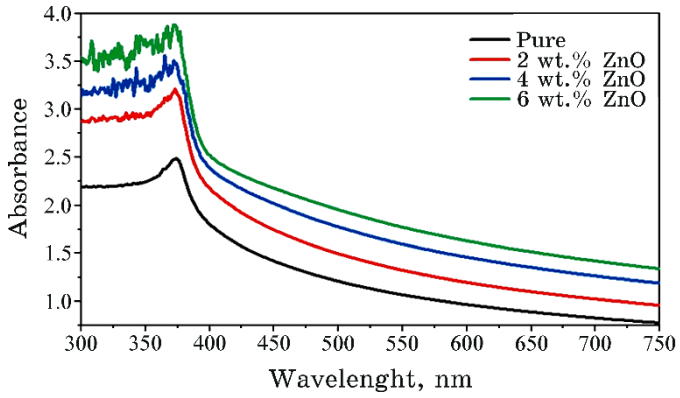

Fig. 1. Absorbance *versus* wavelength for the PVA–ZnO nanocomposites.

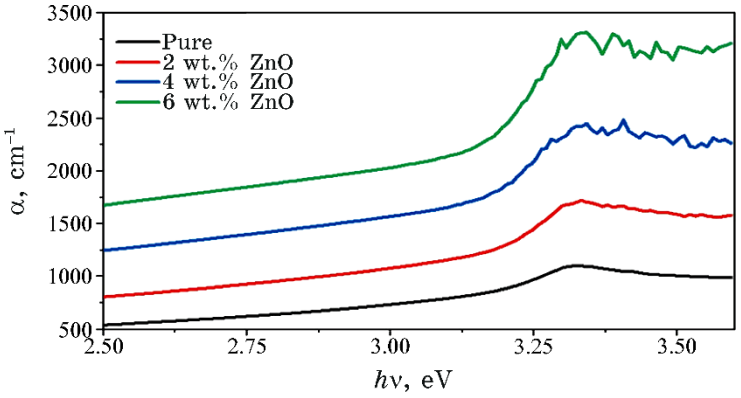

Fig. 2. The photon energy ($h\nu$) and absorption coefficient (α) for ZnO at various concentrations in PVA.

and 2.73 eV; the reason for this decrease is the creation of local bands due to the increase in the amount of the nanomaterial ZnO in the polymer.

This nanocomposite can be used as a humidity sensor. These nanocomposites are also used in optical applications [27, 28].

An increase in the concentration of nanomaterials ZnO increased the extinction coefficient, as shown in Fig. 4; since this nanocomposite contains polyvinyl alcohol, the unsaturated carbonyl group attached to ethylene will show a peak in all samples close to 400 nm [8, 19, 21, 29]. Because of the link between them, the extinction-coefficient curve behaviour of the nanocomposites is comparable to the absorption coefficient (see Eq. (3)) [16]. Furthermore, a sharp increase in the extinction coefficient occurred at the absorption edge. These results could be ascribed to both increased absorbance

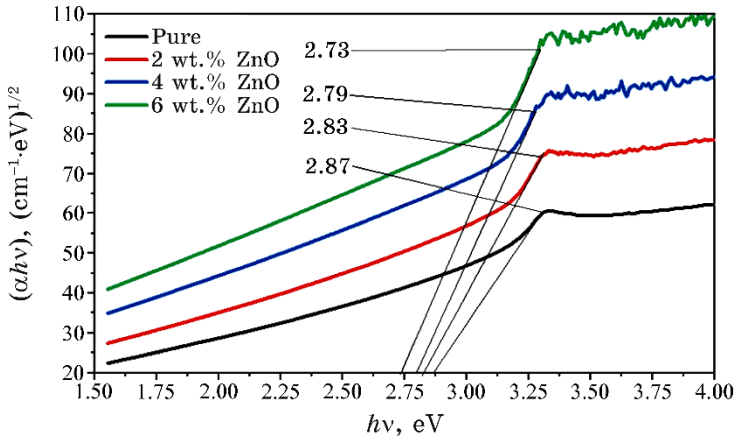

Fig. 3. Optical energy gap for $(\alpha h\nu)^{1/2}$ *versus* the photon energy ($h\nu$) for PVA with different concentrations of ZnO.

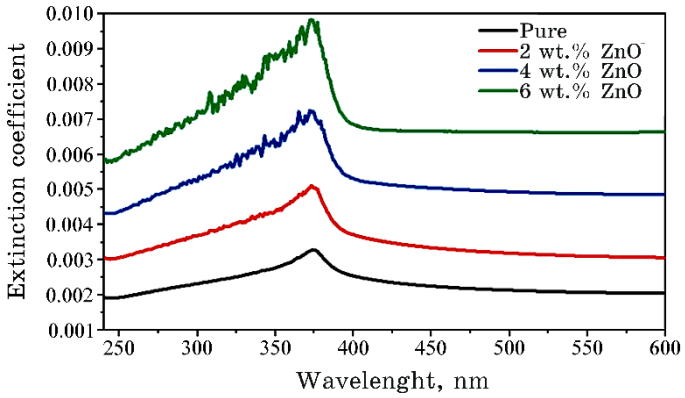

Fig. 4. Extinction coefficient *versus* wavelength for the PVA–ZnO nanocomposites.

because of the transmission phase and increased scattering due to the increase; this finding matches the morphological characteristics of the FE–SEM images [30, 31].

Figure 5 shows that when the concentration of nanomaterials (ZnO) increases, so does the refractive index. The optical energy gap and reflectivity of the films are responsible. The packing density and orientation are related to variations in the n value [32].

The amount, by which a substance slows the speed of light, is proportional to its real component. The imaginary fraction, ε_i, shows how a dielectric absorbs energy from an electric field through dipole motion. As a result of k_0^2 being less than n^2 according to

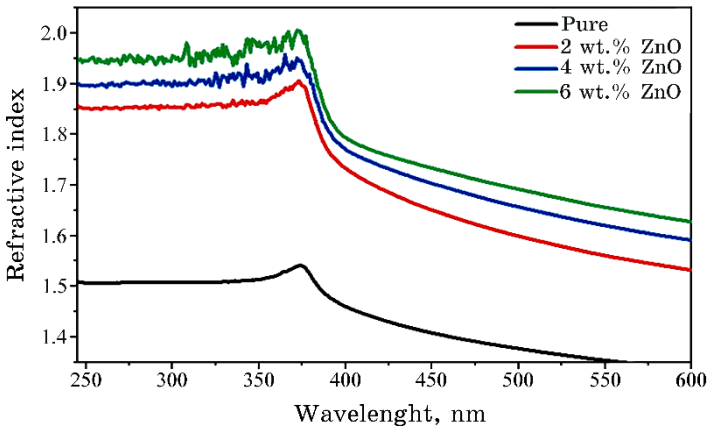

Fig. 5. Refractive index *versus* wavelength for the PVA–ZnO nanocomposites.

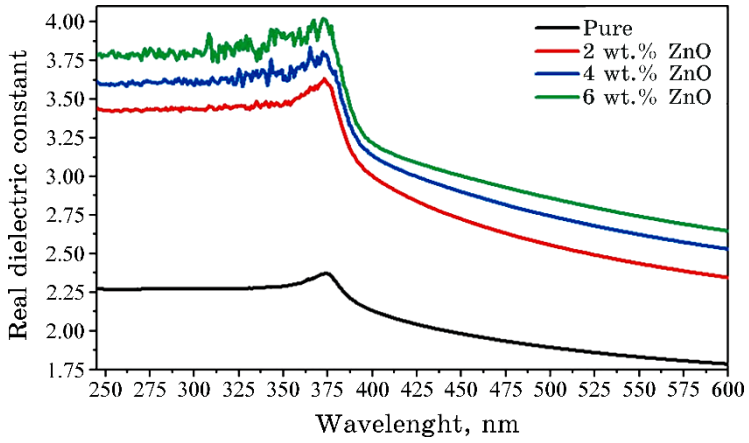

Fig. 6. Real dielectric properties *versus* wavelength for the PVA–ZnO nanocomposites.

Eq. (5), the behaviour of ε_r in Fig. 6 is comparable to the refractive index performance. However, ε_i depends mostly on the value of the extinction coefficient (k_0) according to Eq. (6) [33].

3.2. A.C. Electrical Conductivity

Using Eq. (9), the dielectric constant (ε') of the PVA–ZnO nanocomposites was determined.

Figure 8 shows the dielectric constant of the PVA–ZnO nanocomposites as a function of the frequency. The dielectric constant de-

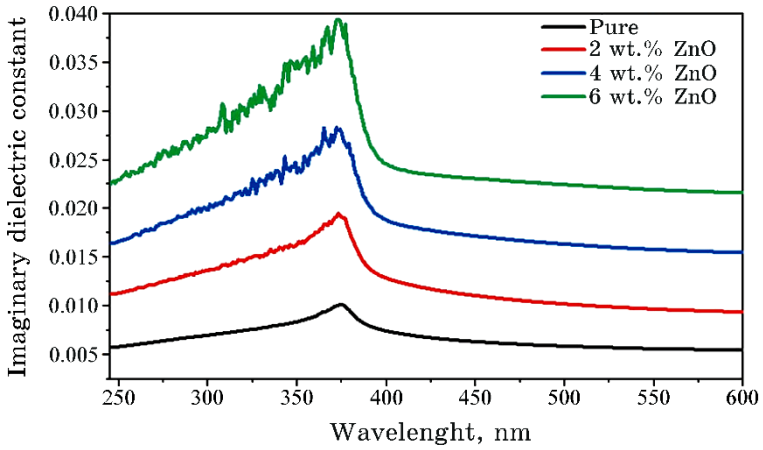

Fig. 7. Imaginary dielectric constant *versus* wavelength for the PVA–ZnO nanocomposites.

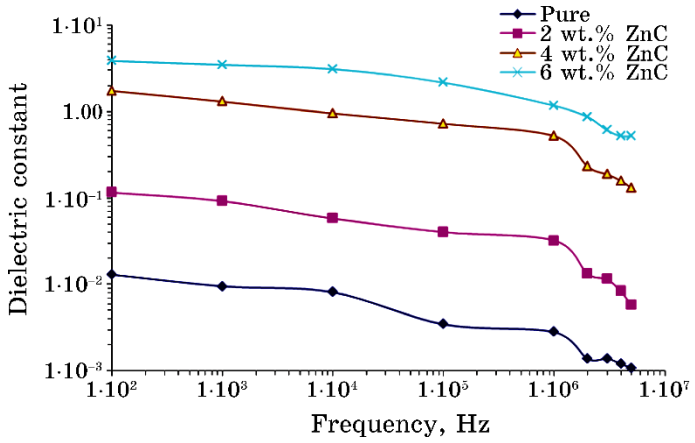

Fig. 8. Dielectric constant *versus* frequency at standard room temperature for the PVA–ZnO nanocomposites.

creases with increasing frequency in all the samples. This phenomenon can be attributed to the dipoles in the nanocomposites turning in the direction of the applied electric field and the reduction of space charges or interfacial polarization to overall polarization [34].

Figure 9 illustrates how the dielectric constant of the PVA–ZnO nanocomposites varies with the number of nanoparticles present at $f = 100$ Hz. This indicates that the dielectric constant of the PVA–ZnO nanocomposites increases as the amount of ZnO nanoparticles increases. It is noted that all nanocomposite samples increase with increasing nanoparticle loading. Interfacial polarization within the

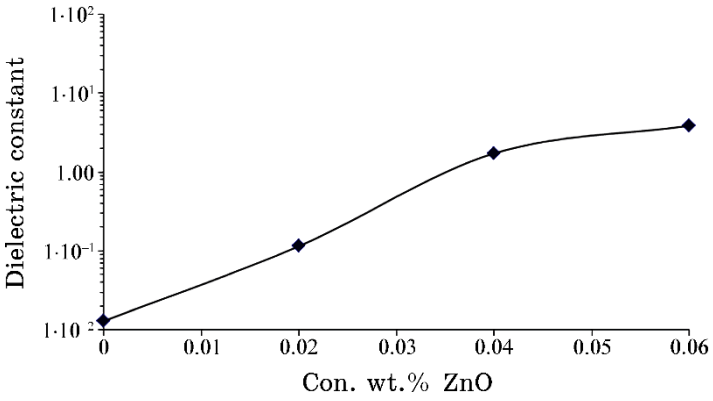

Fig. 9. Impact of ZnO-nanoparticles' content on the dielectric constant of PVA–ZnO nanocomposites at 100 Hz.

nanocomposites in an applied field with an alternating electric field and an increase in charge carriers could be used to characterize these processes [35]. This indicates that the produced nanocomposites have low or low energy loss, making them appropriate for use in pressure sensors and nanoelectronics applications.

The dielectric loss (ε'') was calculated from Eq. (9).

Figure 10 shows the dielectric loss for the PVA–ZnO nanocomposites as a function of frequency. As the frequency increases, the dielectric loss of the PVA–ZnO nanocomposites decreases, which is caused by a decrease in the influence of space charge polarization. The dielectric loss is highest at low frequencies and decreases as the frequency increases. This is because the electric dipoles have adequate time to align with the electric field before changing direction [36].

The effect of ZnO concentration on the dielectric loss of PVA polymer at $f = 100$ Hz is shown in Fig. 11. An increase in the number of nanoparticles causes a rise in the dielectric loss, which is explained by an increase in the number of charge carriers [37]. Clusters are formed when the number of nanoparticles in the nanocomposites is minimal, but when the concentration is high, up to 6 wt.%, they combine to form networks. The dielectric loss of the nanocomposites increases as the amount of ZnO NPs increases, as illustrated in the figures. As the amount of ZnO NPs in the polymer (PVA) increases, so does its dielectric loss, which is explained by the increase in charge carriers for the nanocomposites [38].

To measure the a.c. electrical conductivity of the nanocomposites, Eq. (8) was used. Nanoparticles produce a route network inside the nanocomposite at high concentrations of nanoparticles 6 wt.% for the PVA polymer.

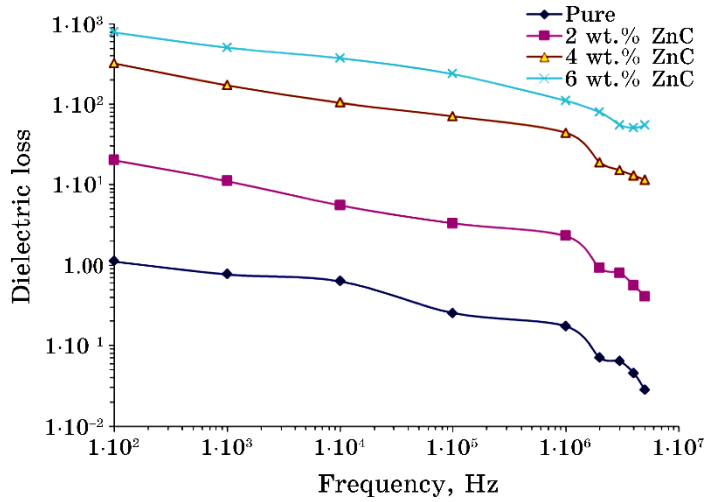

Fig. 10. Dielectric loss *versus* frequency at standard room temperature for the PVA–ZnO nanocomposites.

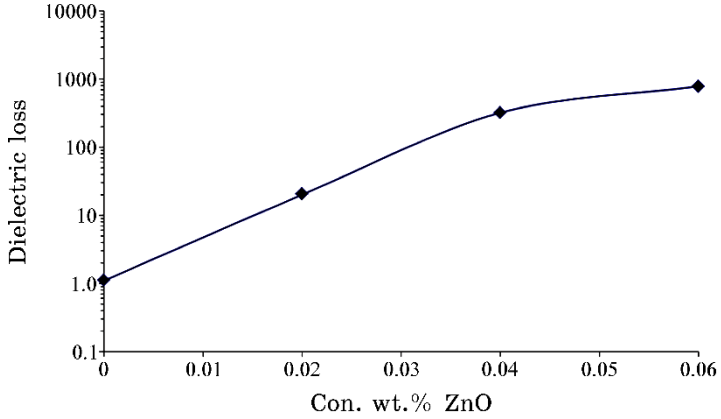

Fig. 11. Effect of ZnO NPs on the dielectric loss of the PVA–ZnO nanocomposites at 100 Hz.

Figure 12 displays the fluctuation in the electrical conductivity of the PVA–ZnO nanocomposites with frequency. As demonstrated in the figures, the electrical conductivity increases as the electric field frequency increases for all the prepared nanocomposites. This behaviour is caused by the hopping process, which moves charge carriers, and space charge polarization, which occurs at low frequencies. For PVA–ZnO nanocomposites, the electrical conductivity increases with increasing frequency due to the enhanced mobility of charge carriers in the high-frequency region [39]. Figure 13 shows

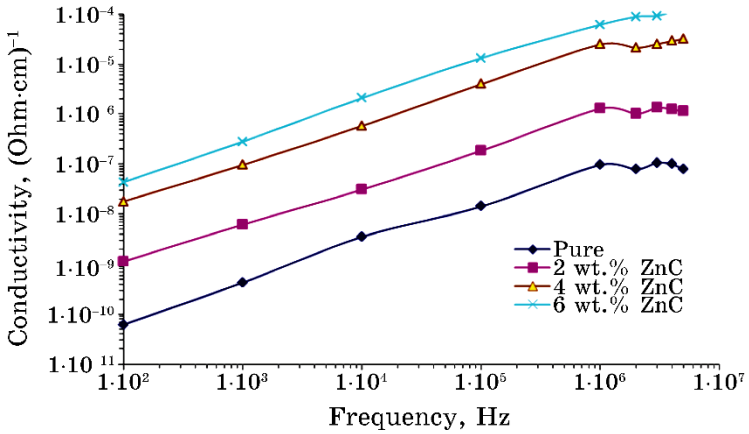

Fig. 12. Electrical conductivity *versus* frequency for the PVA–ZnO nanocomposites.

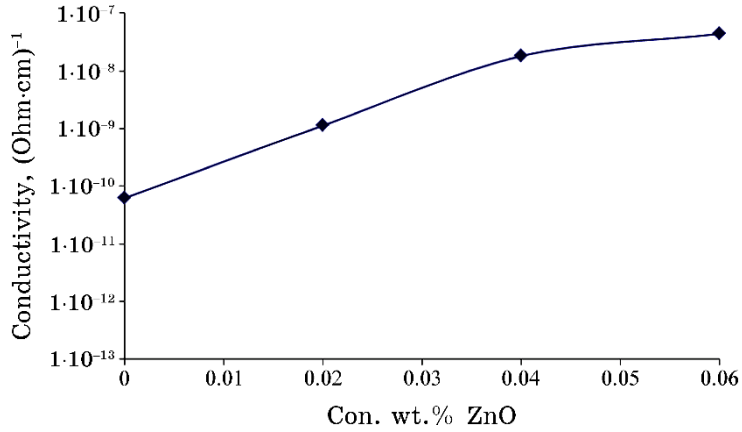

Fig. 13. Effect of ZnO-NPs' filling on the electrical conductivity of nanocomposites at 100 Hz.

how ZnO nanoparticles affect the electrical conductivity of the PVA polymer at 100 Hz. According to the figures, as the concentration of ZnO nanoparticles increased. Because of the composition of the dopant nanoparticles, which gradually reduce the resistance of the nanocomposites and increase the electrical conductivity, the increase in electrical conductivity with increasing ZnO nanoparticle content is attributed to an increase in the number of charge carriers. This finding aligns with the findings of previous studies [40, 41].

Figure 14 shows the measured values of the humidity sensor. The humidity and temperature were maintained at room temperature.

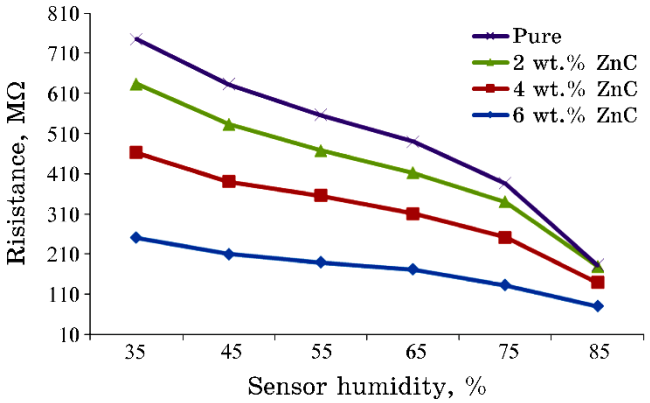

Fig. 14. Relationships between the sensor resistance and humidity.

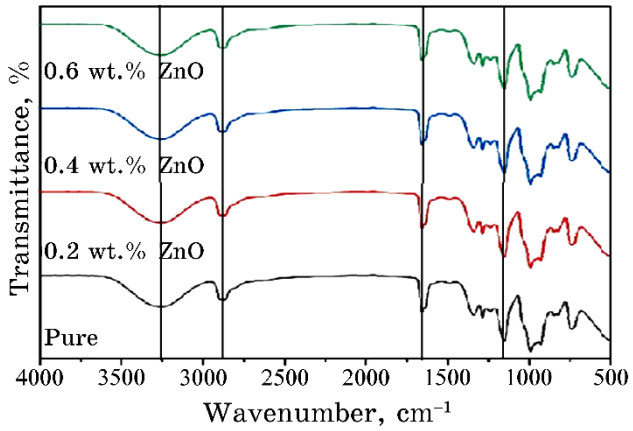

Fig. 15. FT–IR spectrum of the PVA–ZnO nanocomposites.

According to the experimental findings, the humidity sensor exhibited nearly no humidity hysteresis, and its resistance decreased as humidity increased [42]. An increase in the zinc-oxide concentration decreased the resistance level with increasing humidity [43].

3.3. Morphological Properties

The purpose of the FE–SEM examination was to clarify the density and distribution of the nanoparticles in the manufactured polymeric film, as the images showed a homogeneous distribution of ZnO within the polymer. The image also showed that the ZnO nanoparticles appeared to have been coated with the polymeric material (PVA), as shown in Fig. 15 [8]. Increasing the number of ZnO molecules rep-

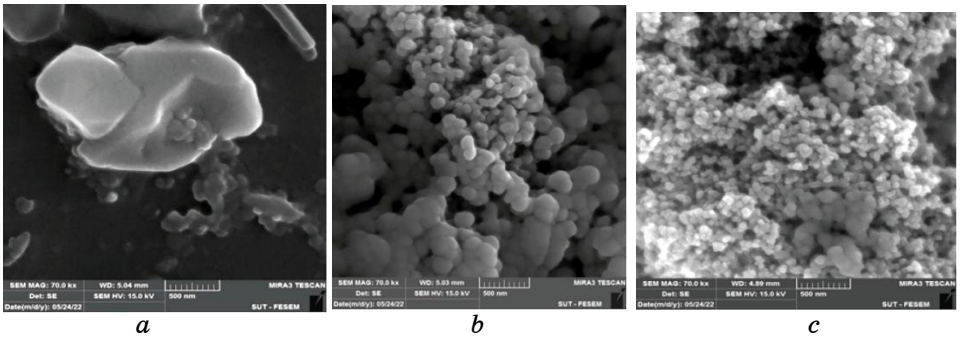

a *b* *c*

Fig. 16. FE–SEM images of (*a*) PVA, (*b*) PVA/0.2 wt.% ZnO, and (*c*) PVA/0.6 wt.% ZnO.

resented in a network in the polymer matrix increases the conductivity due to its ability to accelerate electron motion, which is the main reason for the reduction in the E_g [44].

Other nanomaterials, such as graphene, can be used [45–46].

Figure 16 shows the FT–IR spectrum of the PVA/ZnO nanocomposites; the O–H bond is responsible for the absorption peak observed at 3251.3 cm^{-1} and 2812 cm^{-1}, which indicates the presence of PVA and indicates its identity; these two peaks are attributed to the PVA polymer, which is an aliphatic compound. It traps water from the air, which is typical in humidity sensor applications [8]. The vibration peaks that appeared at 1625.03 cm^{-1} and 1154 cm^{-1} indicate weak Zn–O and ZnO_2 bonds. When ZnO nanomaterials were added to the polymer at various concentrations, some changes were observed in the vibration peaks, and no peak creep was observed. This means that the reaction is physical [7, 8].

4. CONCLUSION

The results showed that the prepared films are homogeneous, and the diffusion of the nanomaterial within the polymer is good, which, in turn, enables the electrons to move more freely. FTIR analyses revealed the highest absorption at 3251.3 cm^{-1} and 2812 cm^{-1} due to the O–H bond, which indicates the presence of PVA. It traps water from the air, which is typical in humidity sensor applications. Additionally, in the UV region, as the number of nanomaterials increases, the energy gap decreases to between 2.87 eV and 2.73 eV, and all the optical constants increase with increasing nanomaterial concentration. Therefore, they can be used as detectors in the UV region. As the frequency and concentration of nanomaterials increase, the dielectric constant, dielectric loss, and

AC electrical conductivity increase.

ACKNOWLEDGMENTS

The authors gratefully acknowledge the technical support provided by Al-Mustaqbal University, University of Babylon, and the Applied Sciences Department, University of Technology, Baghdad, Iraq.

REFERENCES

1. Shehu Sa'ad Abdullahi, Rania Edrees Adam Mohammad, Ahmad Hussaini Jagaba, Haruna Musa, and Abdullahi Haruna Birniwa, *Case Studies in Chemical and Environmental Engineering*, **9**: 100570 (2023); https://doi.org/10.1016/j.cscee.2023.100570
2. Gaurav Choudhary, Jyoti Dhariwal, Moumita Saha, Shruti Trivedi, Manoj K. Banjare, Rahul Kanaoujiya, and Kamalakanta Behera, *Environmental Science and Pollution Research*, **31**, Iss. 7: 10296 (2024); https://doi.org/10.1007/s11356-023-25468-w
3. Sheng Dai, Mengchao Cui, Jiahui Li, and Meng Zhang, *Coatings*, **14**, Iss. 7: 822 (2024); https://doi.org/10.3390/coatings14070822
4. Tawfik A. Saleh, Prakash Parthasarathy, and Muhammad Irfan, *Trends in Environmental Analytical Chemistry*, **24**: e00067 (2019); https://doi.org/10.1016/j.teac.2019.e00067
5. O. Anthony Ogunmefun, B. Lawrence Bayode, T. Jamiru, Peter A. Olubambi, *Journal of Alloys and Compounds*, **960**: 170407 (2023); https://doi.org/10.1016/j.jallcom.2023.170407
6. Aditya Prakash Kanth and Aditya Krushang Soni, *Journal of Cultural Heritage*, **59**: 120 (2023); https://doi.org/10.1016/j.culher.2022.11.010
7. Haifa Mohammed Alghamdi and A. Rajeh, *J. Inorg. Organomet. Polym.*, **32**: 1935 (2022); https://doi.org/10.1007/s10904-022-02322-z
8. Ameen Alwan Mohaimeed and Bahaa H. Rabee, *Opt. Quant Electron.*, **55**: 254 (2023); https://doi.org/10.1007/s11082-022-04523-9
9. Dominic Byrne, Geert Boeije, Ian Croft, Gerd Hьttmann, Gerard Luijkx, Frank Meier, Yash Parulekar, and Gerard Stijntjes, *Tenside Surfactants Deterg.*, **58**, No. 2: 88 (2021); https://doi.org/10.1515/tsd-2020-2326
10. Behnam Eslami, Ismaeil Ghasemi, and Masoud Esfandeh, *Polymers*, **15**, Iss. 14: 3063 (2023); https://doi.org/10.3390/polym15143063
11. Niyaz M. Sadiq, Shujahadeen B. Aziz, and Mohd F. Z. Kadir, *Gels*, **8**, Iss. 3: 153 (2022); https://doi.org/10.3390/gels8030153
12. A. M. Schwan, S. Chwatal, C. Hendler, D. Kopp, J. M. Lackner, R. Kaindl, M. Tscherner, M. Zirkl, P. Angerer, B. Friessnegger, S. Augl, D. Heim, A. Hinterer, M. Stummer, and W. Waldhauser, *Applied Nanoscience*, **13**, Iss. 9: 6421 (2023); https://doi.org/10.1007/s13204-023-02936-w
13. Shaheer Ahmed Khan, Zakaria Mohd Zain, Mohammad Mansoor, M. M. Hasan Mahfuz, Ataur Rahman, Mir Akmam Noor Rashid, and Mohammad Salman Rais, *Materials Today: Proceedings*, **2100**, No. 1: 020045 (2019); https://doi.org/10.1016/j.matpr.2021.05.197

14. Roberto Ambrosio, Amanda Carrillo, Maria L. Mota, Karla de la Torre, Richard Torrealba, Mario Moreno, Hector Vazquez, Javier Flores, and Israel Vivaldo, *Polymers*, **10**, Iss. 12: 1370 (2018); https://doi.org/10.3390/polym10121370
15. Kesong Hu, Dhaval D. Kulkarni, Ikjun Choi, and Vladimir V. Tsukruk, *Progress in Polymer Science*, **39**, Iss. 11: 1934 (2014); https://doi.org/10.1016/j.progpolymsci.2014.03.001
16. Yumnam Bonney Singh, Dipankar Biswas, Rittwick Mondal, Saikat Chattopadhyay, Anindya Sundar Das, Debabrata Mandal, Soumyajyoti Kabi, and Loitongbam Surajkumar Singh, *Materials Today, Communications*, **38**: 108002 (2024); https://doi.org/10.1016/j.mtcomm.2023.108002
17. Dileep Chekkaramkodi, Liya Jacob, Muhammed Shebeeb C, Rehan Umer, and Haider Butt, *Additive Manufacturing*, **86**: 104189 (2024); https://doi.org/10.1016/j.addma.2024.104189
18. Ammar Qasem, Mohamed S. Mostafa, H. A. Yakout, Mona Mahmoud, and E. R. Shaaban, *Opt. Laser Technol.*, **148**: 107770 (2022); https://doi.org/10.1016/j.optlastec.2021.107770
19. Ameen Alwan Mohaimeed and Bahaa H. Rabee, *Annals of Agri-Bio Research*, **27**, Iss. 2: 222 (2022); https://www.researchgate.net/profile/Ameen-Mohaimeed-2/publication/365301579_Influence_of_Natural_Crocus_Dye_on_Morphological_and_Optical_Properties_of_PVATiO_2_Nanocomposite_Prepared_by_the_Spin_Coater_Method/links/636e13832f4bca7fd05054ab/Influence-of-Natural-Crocus-Dye-on-Morphological-and-Optical-Properties-of-PVA-TiO-2-Nanocomposite-Prepared-by-the-Spin-Coater-Method.pdf
20. Torki A. Zughaibi, *Sustainable Chemistry and Pharmacy*, **39**: 101566 (2024); https://doi.org/10.1016/j.scp.2024.101566
21. Ameen Alwan Mohaimeed and Bahaa H. Rabee, *Annals of Biology*, **39**, Iss. 1: 108 (2023); https://agribioj.com/wp-content/uploads/2019/11/108-111.pdf
22. Hui Tang, Changjin Yang, Li Qin, Lei Liang, Yuxin Lei, Peng Jia, Yongyi Chen, Yubing Wang, Yue Song, Cheng Qiu, Chuantao Zheng, Xin Li, Dabing Li, and Lijun Wang, *Sensors*, **23**, Iss. 17: 7326 (2023); https://doi.org/10.3390/s23177326
23. Ravi Kumar, Rajiv Kumar, Anil Arya, Pawan K. Sharma and Annu Sharma, *Braz. J. Phys.*, **52**, Iss. 5: 1 (2022); https://doi.org/10.1007/s13538-022-01170-z
24. C. R. Mariappan and G. Govindaraj, *Mater. Sci. Eng. B*, **94**: 82 (2002); https://doi.org/10.1016/S0921-5107(02)00083-1
25. C. Ravi Dhas, R. Venkatesh, R. Sivakumar, A. Moses Ezhil Raj, and C. Sanjeeviraja, *Opt. Mater.*, **72**: 717 (2017); https://doi.org/10.1016/j.optmat.2017.07.026
26. Mohamed Oubaha, Salem Elmaghrum, Robert Copperwhite, Brian Corcoran, Colette McDonagh, and Arnaud Gorin, *Opt. Mater.*, **34**: 1366 (2012); https://doi.org/10.1016/j.optmat.2012.02.023
27. Y. Al-Hadeethi, M. I. Sayyed, and Y. S. Rammah, *Ceram. Int.*, **45**, No. 16: 20724 (2019); https://doi.org/10.1016/j.ceramint.2019.07.056
28. Hyuk-Joon Youn, Tomohiro Sogabe, Clive A. Randall, Tom R. Shrout, and Michael T. Lanagan, *J. Am. Ceram. Soc.*, **84**, No. 11: 2557 (2001); https://doi.org/10.1111/j.1151-2916.2001.tb01053.x
29. Raghvendra Singh Yadav and Ivo Kuřitka, *Advances in Colloid and Interface*

Science, **326**: 103137 (2024); https://doi.org/10.1016/j.cis.2024.103137
30. Sze-Mun Lam, Jin-Chung Sin, Ahmad Zuhairi Abdullah and Abdul Rahman Mohamed, *Water Air Soil Pollut.*, **224**: 1 (2013); https://doi.org/10.1007/s11270-013-1565-6
31. Doaa Domyati, *Optical Materials*, **152**: 115479 (2024); https://doi.org/10.1016/j.optmat.2024.115479
32. R. Syafinar, N. Gomesh, M. Irwanto, M. Fareq, and Y. M. Irwan, *Energy Proc.*, **79**: 799 (2015); https://doi.org/10.1016/j.egypro.2015.11.569
33. Mohanad H. Meteab, Ahmed Hashim and Bahaa H. Rabee, *Opt. Quantum Electron.*, **55**: 187 (2023); https://doi.org/10.1007/s11082-022-04447-4
34. P. Lokanatha Reddy, Kalim Deshmukh, K. Chidambaram, Mohammad M. Nazeer Ali, Kishor Kumar Sadasivuni, Y. Ravi Kumar, R. Lakshmipathy, and S. K. Khadheer Pasha, *J. Mater. Sci. Mater. Electron.*, **30**, Iss. 4: 4676 (2019); https://doi.org/10.1007/s10854-019-00761-y
35. L. H. Gaabour, *AIP Adv.*, **11**, Iss. 10: 105120 (2021); https://doi.org/10.1063/5.0062445
36. Chainarong Srivabut, Thanate Ratanawilai, and Salim Hiziroglu, *Journal of Material Cycles and Waste Management*, **23**, Iss. 4: 1503 (2021); https://doi.org/10.1007/s10163-021-01230-7
37. S. Ju, M. Chen, H. Zhang, and Z. Zhang, *Express Polym. Lett.*, **8**, Iss. 9: 682 (2014); doi:10.3144/expresspolymlett.2014.71
38. Xingyi Huang, Shen Wang, Ming Zhu, Ke Yang, Pingkai Jiang, Yoshio Bando, Dmitri Golberg, and Chunyi Zhi, *Nanotechnology*, **26**, Iss. 1: 015705 (2014); doi:10.1088/0957-4484/26/1/015705
39. H. Shivashankar, Kevin Amith Mathias, Pavankumar R. Sondar, M. H. Shrishail, and S. M. Kulkarni, *J. Mater. Sci. Mater. Electron.*, **32**, Iss. 20: 28674 (2021); https://doi.org/10.1007/s10854-021-07242-1
40. Roshini Gunasekaran and Julie Charles, *Polymer-Plastics Technology and Materials*, **63**, Iss. 6: 716 (2024); https://doi.org/10.1080/25740881.2024.2302539
41. Monika Barala, Jyoti Jaglan, Devendra Mohan, Sujata Sanghi, and Parveen Sharma, *Brazilian Journal of Physics*, **53**, Iss. 1: 29 (2023); https://doi.org/10.1007/s13538-022-01234-0
42. Ming-Zhi Yang, Ching-Liang Dai, and Wei-Yi Lin, *Sensors*, **11**: 8143 (2011); https://doi.org/10.3390/s110808143
43. Peng Li, Shuguo Yu, and Hongyan Zhang, *Sensors*, **21**, Iss. 3: 857 (2021); https://doi.org/10.3390/s21030857
44. M. M. Abdelhamied, A. Atta, A. M. Abdelreheem, A. T. M. Farag, and M. A. El Sherbiny, *Inorgan. Chem. Commun.*, **133**: 108926 (2021); https://doi.org/10.1016/j.inoche.2021.108926
45. Salah Abdul Mahdi Khudair and Ameen Alwan Mohaimeed, *Neuro Quantol.*, **18**, Iss. 9: 87 (2020); doi:10.14704/nq.2020.18.9.NQ20221
46. Ammar Abd Ali Najm, Saif M. Alshrefi, Zaid L. Hadi, Ehssan Al-Bermany, and Ameen Alwan Mohaimeed, *Silicon*, **16**: 4227 (2024); https://doi.org/10.1007/s12633-024-02997-8